MULTIPLE GENERATIONS OF SILICA IN THE TOLHUACA GEOTHERMAL SYSTEM, SOUTHERN CHILE, CONSTRAINED USING SEM-BASED CATHODOLUMINESCENCE IMAGING AND FLUID INCLUSIONS DATA

Bernardita Alvear[1,2], Diego Morata[1,2], Daniel Moncada[1,2], Martin Reich[1,2] and Andrés Gómez[1]

[1]Department of Geology, Faculty of Physical and Mathematical Science, Universidad de Chile, Plaza Ercilla 803, Santiago, Chile.

[2]Andean Geothermal Center of Excellence (CEGA), Universidad de Chile, Plaza Ercilla 803, Santiago, Chile.

balvear@ug.uchile.cl

Keywords: *Andean Geothermal System, SEM-CL, mineral texture, fluid inclusions, boiling, flashing.*

ABSTRACT

Imaging of silica minerals by scanning electron microscopy (SEM)-Cathodoluminescence (CL) reveals unique textures, and combined with fluid inclusion (FI) studies, these data can be used to constrain the evolution of geothermal systems. Here we present a SEM-CL and FI study of silica minerals that is aimed at increasing our understanding of the active Tolhuaca Geothermal System (TGS).

SEM-CL observations in representative samples collected from a ~1000m long borehole reveal complex textural features and growth patterns in silica veins. Four silica generations were identified (G1-G4). The G1 group is characterized by colloform silica with bands of varying CL intensity. The G2 group shows jigsaw textures with bright-CL contrast, while euhedral quartz from the G3 group shows oscillatory zoning-CL and primary Fluid Inclusion Assemblages (FIAs) with liquid-rich inclusions and consistent liquid-to-vapour ratios. Finally, the G4 group is composed of massive silica with a homogeneous intermediate-CL contrast and isolated quartz crystals that are individually broken within the massive silica and form brecciated textures. These crystals show secondary FIAs that co-exist with liquid-rich and vapour-rich inclusions. FI microthermometric measurements from veins show a range of homogenization temperatures (T_h) divided into two groups. Primary FIAs in group 3 in quartz homogenize from 170-293°C and the ice melting temperatures (T_m) range from -3.15 to -1.45°C. The G4 secondary FIAs show T_h from 234 to 242°C and a T_m of -1.15°C.

The recognized silica generations can be correlated with the different stages of evolution previously proposed by Sánchez-Alfaro et al. (2016) for the TGS: A stage-S1 characterized by flashing followed by boiling (S2), and a S3-stage dominated by non-boiling processes that preceded a final episode of brecciation of silica minerals and boiling (S4). The detailed SEM-CL characterization of silica paragenesis at the TGS is in agreement with previous studies of the TGS and confirms that these mineralogical studies provide useful information to refine conceptual models of geothermal systems.

1. INTRODUCTION

Silica phases, together with carbonates, are ubiquitous minerals in hydrothermal systems. Moreover, quartz is normally the main gangue phase and sometimes the only mineral that precipitates (Dong et al., 1995). Consequently, silica phases and carbonates will be the main minerals recording the evolution of these systems.

Some characteristics of silica minerals, like their morphology, crystal structure, chemical composition and physical chemical properties, might reflect different hydrothermal conditions during vein growth (Dong et al., 1995). Quartz veins show variable textures that provide significant information on the nature of precursor fluid-filled cracks under crustal conditions (e.g. fluid chemistry, fluid flow, etc.). These textures reflect the various crystallization mechanisms that operate in fluid-filled cracks (Okamoto et al., 2010). The formation of hydrothermal calcite in a geothermal system is governed by boiling, dilution and condensation (Simmons and Christenson; 1994). These processes are reflected by different textures: bladed, replacement and rhombic calcite.

In the last decades, cathodoluminescence (CL) has been used to unravel other mineralogical features that for other conventional methods were difficult or impossible to determine (Bignall et al., 2004). CL is an important property of quartz, depending on intrinsic (lattice defects) or extrinsic (trace elements) defects (Götze et al., 2001). Several parameters may influence the incorporation of defects into hydrothermal quartz (Allan and Yardley; 2007), including fluid chemistry (Ramseyer and Mullis, 1990; Monecke et al., 2002; Götze et al., 2004; Landtwing and Pettke, 2005), precipitation rate (Ihinger and Zink, 2000), crystal orientation (Ramseyer and Mullis, 1990), pressure and temperature (Dennen et al., 1970; Wark & Watson, 2006). Therefore, the CL response of quartz and other silica phases is quite sensitive to any changes of these parameters.

A complementary tool used to unravel the evolution of hydrothermal systems involves the study of fluid inclusions. Fluid inclusions are small volumes of fluid trapped within a crystal during its original growth or during subsequent healing of fractures in the presence of fluid. The study of fluid inclusions provides a wide range of data, some of which are unavailable from any other sources (Roedder, 1984). For example, fluid inclusions provide information about temperature, pressure, density and composition of the fluids that existed in the past.

The aim of this study is to understand the evolution of the Tolhuaca Geothermal System by combining SEM-CL observations and fluid inclusions data in silica minerals and carbonates, identifying the main processes during hydrothermal alteration.

2. GEOLOGICAL SETTING AND BACKGROUND

The Tolhuaca Geothermal System (TGS) is located on the northwest flank of the Tolhuaca volcano, southern Chile (Figure 1). Geothermal exploration and borehole logging have revealed the existence of a 1.5 km deep, high enthalpy reservoir with liquid-saturated conditions, temperatures up to 300ºC and a strong meteoric water component (Melosh et al., 2012). A steam-heated aquifer at shallow depths, between 120 m and 230 m (160ºC), overlies the main reservoir and controls the nature of most of the hot springs and surface manifestations (Melosh et al., 2010; Melosh et al., 2012).

Rocks from the Tolhuaca Tol-1 borehole are mainly lavas and related breccias, volcaniclastics and minor tuffs (Lohmar, et al., 2012). Rocks are mainly of basaltic andesite compositions, although whole-rock chemistry varies from basalts to dacites. Hialoclastites and pillow breccias have been described at different levels, indicating that the erupted lavas were in contact with glacial ice and/or water at certain time periods (Lohmar et al., 2012).

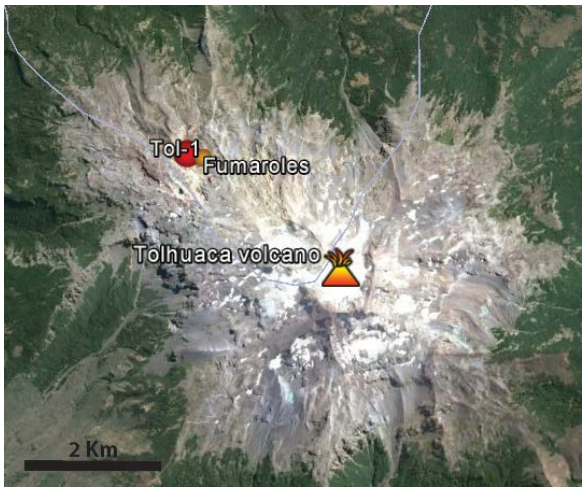

Figure 1: The Google Earth satellite image of the study area shows location of the Tolhuaca volcano, the Tol-1 drill core and fumaroles of the TGS. Google Earth, 2016.

Surface hydrothermal alteration shows extended acid-sulfate style mineralization near the summit of the Tolhuaca volcano. Argillic alteration is scattered at the surface in the main part of the geothermal prospect as confirmed by X-ray diffraction (XRD) and infra-red hyperspectral analyses of surface samples. Three silica sinter terraces and surficial silica deposits are present in the area (Melosh et al., 2012). Based on thin section and XRD analyses of the Tol-1 borehole, Melosh et al. (2012) defined an upper zone of argillic alteration (20 to 450m), a transitional phyllic zone (450 to 650 m), and a deeper zone of propylitic alteration (>650 m). Argillic alteration facies are characterized by Fe-oxides + chlorite + calcite + clay ± quartz ±pyrite, whereas high-temperature propylitic alteration is generally characterized by chlorite + epidote + calcite ± pyrite ±quartz ± zeolites mineral assemblages (Melosh et al., 2010).

More recently, Sánchez-Alfaro et al. (2016) studied the physical, chemical and mineralogical evolution of the TGS, using hydrothermal alteration, borehole fluid samples and fluid inclusion analysis. The authors suggested there were three hydrothermal alteration zones at Tolhuaca: a shallow argillic alteration zone (0 to 300 m), characterized by clay minerals + Fe-oxides + stilbite; an intermediate subpropylitic alteration zone (300 to 670 m), dominated by widespread and pervasive occurrence of interlayered chlorite-smectite and illite; and a deep propylitic alteration zone (670 to 1073 m), characterized by the occurrence of epidote and chlorite.

Moreover, Sánchez-Alfaro et al. (2016) distinguished four types of aqueous, two-phase (liquid-vapor) fluid inclusions: 1) 10-30 µm sized FI hosted in massive or euhedral quartz, typically oval or with negative shapes, 2) 10-120 µm sized FI hosted in lattice bladed calcite, and typically with an oval, elongated or negative crystal shape, 3) 20-100 µm sized FI hosted in syn-kinematic or late calcite, and with typically negative crystal shape and 4) pseudosecondary FI that crosscut quartz crystal. All of these FI types were associated with different stages of hydrothermal evolution. The homogenization temperatures range from ~130 to 300ºC. The first ice melting temperatures were close to -23ºC, suggesting the presence of NaCl-H_2O dominated the fluids. The final ice melting temperature range from 0.0 and -2.3ºC, corresponds to salinities that range from 0 to 3.8 wt.% eq. NaCl. The presence of substantial concentrations of CO_2 in the FI was excluded because no clathrate melting was observed. Heating, non-boiling, boiling, flashing, brecciation and fluid mixing are processes present in the hydrothermal evolution proposed by Sanchéz-Alfaro et al. (2016).

3. METHODS

In the present work, we studied 20 samples from the Tol-1 drill core of TGS. Samples were selected at different depths and contained visible silica and/or calcite filled veins.

Transmitted light microscopy was used to distinguish minerals, textures in calcite, and silica minerals from samples at different depths. Textural characterization described by Dong et al. (1995) and Moncada et al. (2012) was used.

Petrography of Fluid Inclusion Assemblages (FIAs) technique includes dominant phases, sizes, shapes and hosting minerals featuring. Following detailed petrographic examination of the samples, 7 FIAs (representing 31 total fluid inclusions) were selected for microthermometric analysis. Inclusions were measured using a Linkam THMSG 600 heating/cooling stage mounted on a standard petrographic microscope. The stage was calibrated using synthetic fluid inclusion standards (Sterner and Bodnar, 1984). The precision and accuracy of measured homogenization temperatures are estimated to be ±1.0 °C and the precision and accuracy of ice-melting temperatures are estimated to be ±0.1 °C.

A scanning electron microscope (SEM) FEI Quanta 250 coupled with a cathodoluminescence Centaurus detector was used to reveal different textures of silica minerals. Different patterns, like growth zones, breccia minerals, etc., can be observed and recognized by this technique. All analyses were undertaken at the Andean Geothermal Center of Excellence (CEGA), Department of Geology, Universidad de Chile in Santiago.

4. RESULTS

4.1 Textural study

Detailed textural observations were focused on silica polymorphs and calcite. Figure 2 shows the occurrence of the different textures observed at Tolhuaca drill core Tol-1.

The most common mineral textures are colloform silica and rhombic calcite (93 and 87%, respectively). They are present in the three zones of the drill core reported by Sanchez et al. (2016). The colloform silica texture is characterized by rounded or botryoidal morphologies that occur in continuous bands (Rogers, 1918). Henley and Hughes (2000) suggest that this texture is associated with boiling or flashing. The rhombic calcite texture is characterized by blocky calcite with a varying grain size (<5 mm), and is not associated with boiling (Moncada et al., 2012) and/or any significant mineralization process (Dong and Zhou, 1996). Jigsaw silica is the third most common texture (60%) and is visible in the upper, transitional and deeper zones. Jigsaw textures in silica are commonly described as aggregates of microcrystalline quartz crystals with interpenetrating grain boundaries (Dong et al. 1995). This texture has been interpreted as a result of amorphous silica or massive chalcedony recrystallization (Dong et al., 1995).

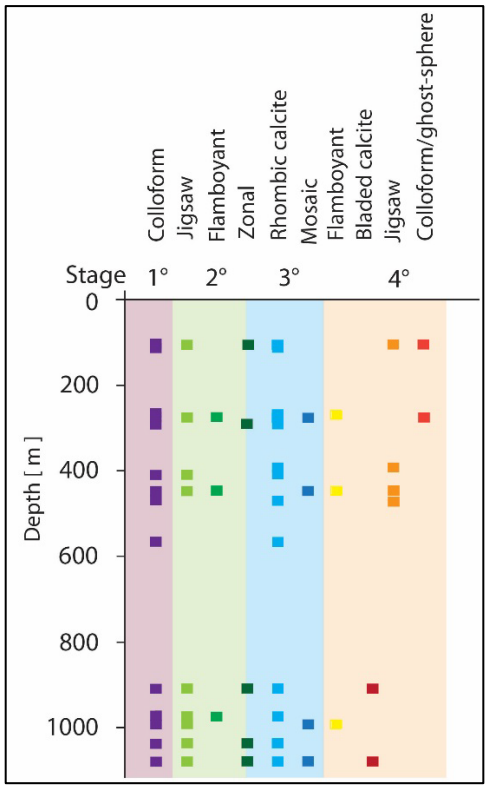

Figure 2: Textural features of silica and carbonate minerals identified in samples from Tol-1 drill core at Tolhuaca. Textural features are associated with four stages of hydrothermal alteration.

Less frequently, flamboyant silica, zonal quartz, mosaic quartz, ghost-sphere silica and bladed calcite textures are recognized in the Tolhuaca samples. Flamboyant and zonal quartz are found in the upper, transitional and deeper levels. The former shows radial extinction when observed under crossed polars (Dong et al. 1995; Moncada et al., 2012). This has been associated with silica gel produced when supersaturation occurs in response to a rapid pressure drop, leading to precipitation of amorphous silica (Henley and Hughes, 2000). Zonal quartz displays alternating clear and milky zones within individual crystals (Dong et al., 1995). This texture requires the hydrothermal fluid to be slightly saturated with respect to quartz, suggesting there have been slow changes in fluctuating conditions during crystal growth (Dong et al., 1995). Mosaic quartz corresponds to aggregates of quartz crystals >10 µm in size with interpenetrating grain boundaries associated with fluids that are slightly saturated with respect to quartz. Ghost sphere silica occurs in the upper parts of the Tol-1 drill core. This texture is described as cloudy spheres of microcrystalline quartz (Dong et al., 1995) and is usually deposited from colloidal amorphous silica (Moncada et al., 2012), associated with boiling. Bladed calcite is present in the deeper parts of the drill core. This is characterized by elongated crystals of calcite and is frequently associated with boiling (Simmons and Christenson, 1994).

Following our textural study, it is possible to distinguish two paragenetic sequences: The first sequence is characterized by colloform silica, followed by jigsaw silica, mosaic quartz and flamboyant silica and finally jigsaw silica. The second sequence was described by colloform silica, followed by jigsaw silica, zonal quartz, continuing to rhombic calcite and bladed calcite and ending with jigsaw quartz.

4.2 Fluid inclusions study

The petrography study was made from nine samples containing quartz and calcite veins at different depths. Primary and secondary Fluid Inclusion Assemblages were divided in four clusters (C1, C2, C3 and C4) based on their petrographic features (Figure 3).

The C1 group of fluid inclusions was characterized by primary FIAs hosted in colloform silica. The C2 group includes primary fluid inclusion assemblages consisting of coexisting liquid-rich and vapour-rich inclusions in the center of quartz crystals. The C3 group was defined as primary FIA containing liquid-rich fluid inclusions on the edge of zonal quartz and in rhombic calcite (Figures 3.A and 3.B). Finally, the C4 group corresponds to primary FIAs that consist of coexisting liquid-rich and vapour-rich inclusions in bladed calcite (Figures 3.C and 3.D) and secondary FIAs of coexisting liquid-rich and vapour-rich inclusions in mosaic quartz (Figures 3.E and 3.F) in association with jigsaw quartz. Microthermometrical measurements were made only in groups C3 and C4. Inclusions from the C1 group were avoided because FIAs are hosted in colloform silica, representing recrystallization features (Moncada et al., 2012) and hence do not record the conditions of formation. Measurements in inclusions of the C2 group were not conducted because FIAs are small.

The homogenization temperatures (T_h) and final ice melting temperatures (Table 1) are plotted as a function of depth (Figure 4). The presence of CO_2 was not observed since no phase change was observed at -56.7ºC. It is possible to recognize cooling and heating processes from these data. The FIAs show a final ice melting temperature between -1.1 and -3.1, corresponding to salinities between 1.9 and 5.1 wt% NaCl equiv.

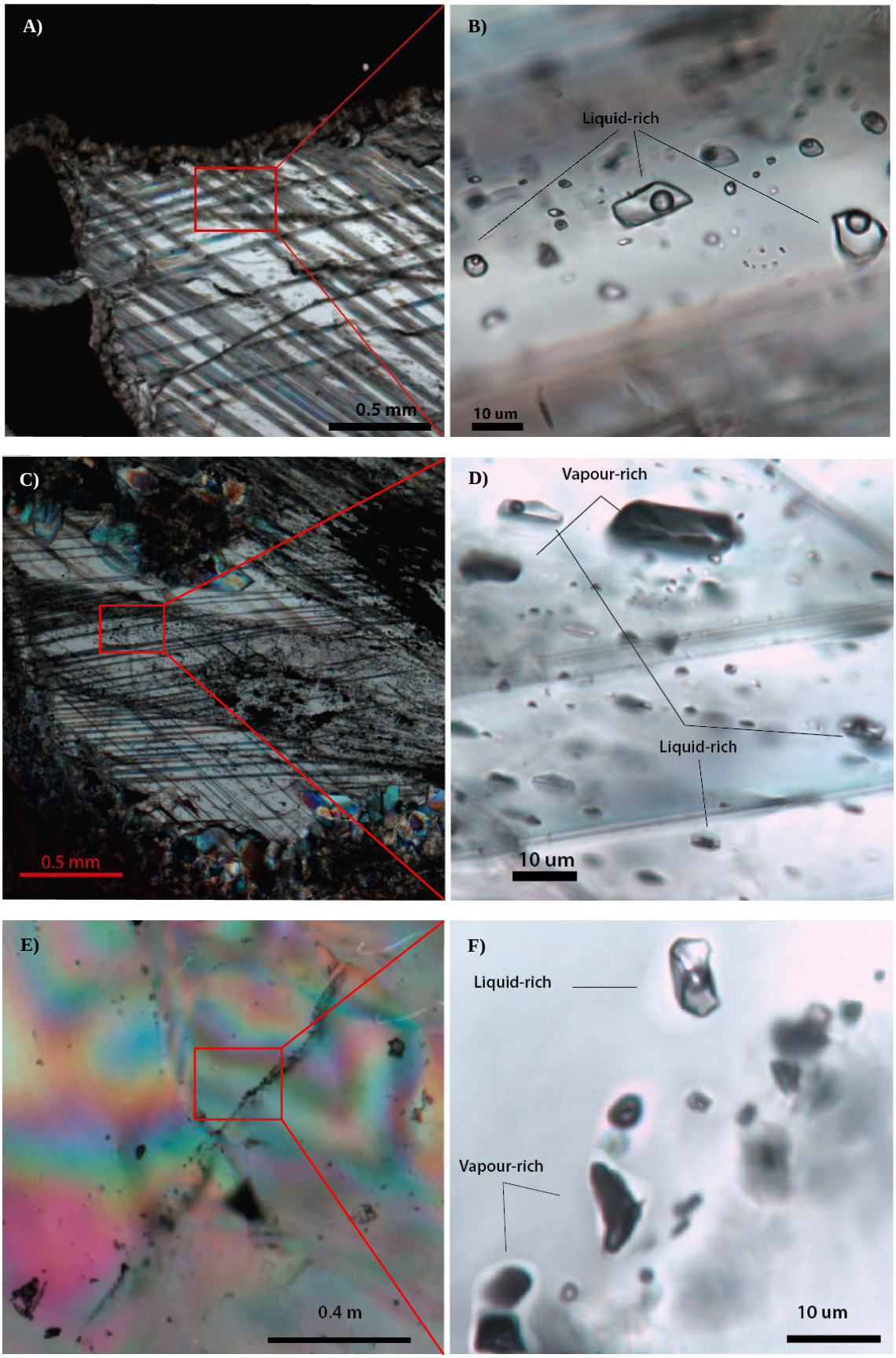

Figure 3: Microphotographs showing textures and FIAs groups. A) Rhombic calcite texture. B) Primary liquid-rich FIAs in rhombic calcite. C) Bladed calcite texture. D) Primary vapour-rich inclusions coexisting with liquid-rich FIAs in bladed calcite. E) Mosaic quartz texture. F) Secondary vapour-rich inclusions coexisting with liquid-rich FIAs cutting mosaic quartz.

Depth (m)	Nª	Homogenization temperature (ºC)	Final ice melting temperature (ºC)	Salinity (wt% NaCl)	Notes
104	4	170 to 174	-3.1	5.1	Primary FIA in rhombic calcite
447	4	234 to 242	-1.1	1.9	Secondary FIA in mosaic quartz. Figures 3.E and 3.F
909	6	269-278	-2.3 to -2.2	3.9 to 3.7	Primary FIA in zonal quartz.
	7	230-253	-1.7	2.9	Primary FIA in rhombic calcite. Figures 3.A and 3.B
	4	218-222	-1.4	2.4	Primary FIA in rhombic calcite. Figures 3.A and 3.B
1073	2	292 - 293	-1.4	2.4	Primary FIA in comb quartz.
	4	260-269	-1.8	3.1	Primary FIA in bladed calcite. Figures 3.C and 3.D

Table 1: Data of FIAs at different depths.

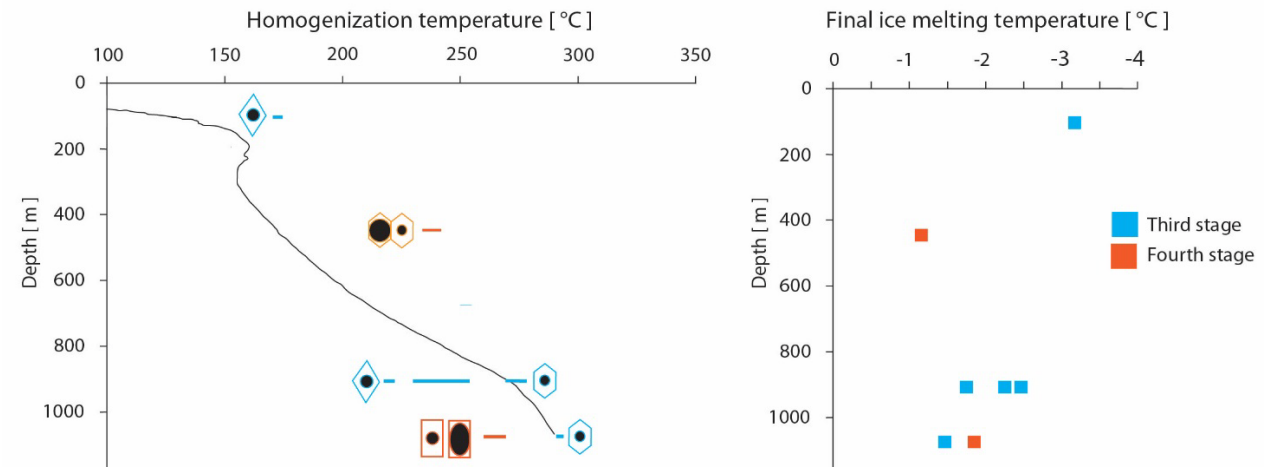

Figure 4: Homogenization temperature and final ice melting temperature plotted as a function of depth temperature in calcite (rhombic shape) and silica (hexagonal shape) of C3 (light blue) and C4 (orange) stages. The black curve represents the present-day temperature profile of the well, as reported by Sánchez-Alfaro et al. (2016).

4.3 SEM-CL study

Textural observations by SEM-CL imaging were performed in two quartz-filled veins at different depths (447 and 992 m depths). It was possible to observe a wide variety of morphologies along the vein, with different CL-intensities. Four silica generations were distinguished based on CL response and texture (G1 to G4).

The G1 group was characterized by botryoidal silica bands of oscillatory contrast in CL and ranged in size between 5 and 225 µm. This group is associated with colloform texture. The G2 group shows small quartz crystals, with interpenetrating grain boundaries along with heterogeneous bright and medium CL associated with a jigsaw texture. The G3 group was characterized by oscillatory zoning developed in euhedral quartz. This group was present in the same place as mosaic quartz. Primary liquid-rich FIAs are present (C3) in this host. Finally, the G4 group is composed of massive silica, with a homogeneous, intermediate CL contrast. Isolated quartz crystals of G3 are individually broken within the massive silica and form brecciated textures, that are cryptic and not visible with conventional SEM methods (e.g. secondary electron or back scattered electron images). Vapour-rich inclusions coexisting with liquid-rich FIAs were linked to this particular generation. It is important to note that the G4 group texture can co-exist with jigsaw and flamboyant textures, but in some samples it is only perceptible using SEM-CL imaging.

Based on SEM-CL imaging it is possible to distinguish the following paragenetic sequence: a colloform silica (G1), followed by jigsaw silica (G2) and zoning euhedral quartz (G3), ending with massive silica (G4, Figure 5).

5. DISCUSSION

The mineralogical and textural observations of silica and calcite, coupled with SEM-CL imaging, revealed at least four stages of geothermal evolution (S1, S2, S3 and S4) in close agreement with Sánchez-Alfaro et al. (2016).

The stage S1 is represented by colloform textures and is associated with flashing, while the following S2 stage is

represented by jigsaw and zonal quartz textures. Zonal quartz showed primary FIA consisting of coexisting liquid-rich and vapour-rich inclusions (C2 group). These observations were believed to be linked to boiling. The S3 stage is texturally represented by rhombic calcite, mosaic texture, zoning of euhedral quartz (SEM-CL imaging) and primary liquid-rich FIAs (C3 group), and are associated with non-boiling processes. These features indicate that the hydrothermal fluid was slightly saturated with respect to quartz, resulting in smooth changes reflected by oscillatory zoning of quartz in veins. Data from FIAs show that the system was cooled during this stage. The final episode S4 involved a brecciation of silica minerals due to boiling. SEM-CL imaging revealed broken zoned quartz crystals and homogeneous massive silica (associated with quick precipitation). Furthermore, FIAs consisting of coexistent liquid-rich and vapour-rich inclusions (C4 group) are associated with the same stage, supporting this idea.

A

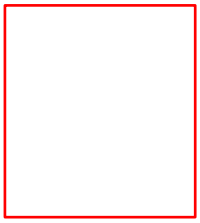

G3

B

C

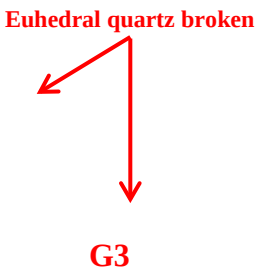

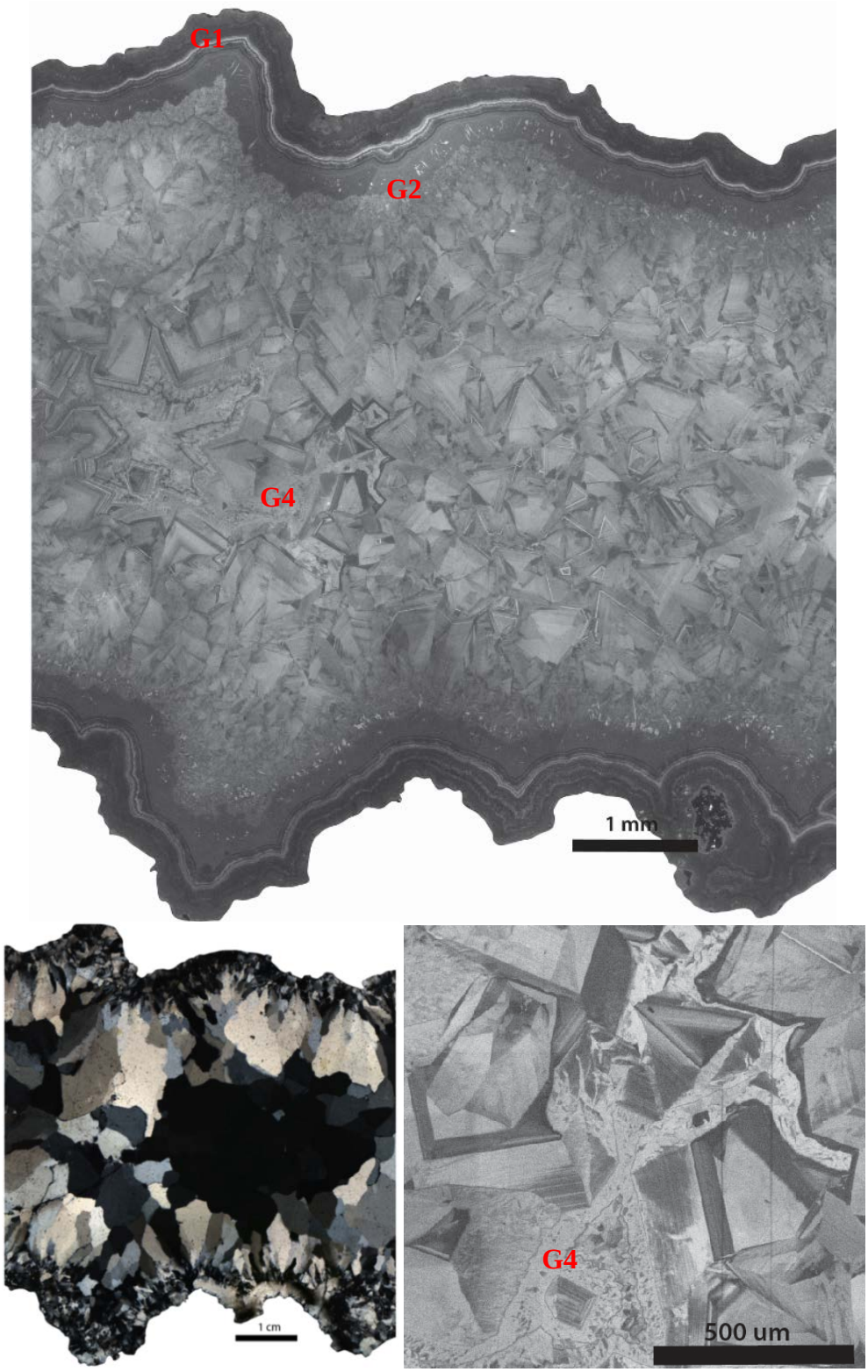

Figure 5: A) SEM-CL image of a silica vein (447 m, Tol-1). The image shows four silica generations: colloform silica (G1), jigsaw silica (G2), zoned euhedral quartz (G3) and massive silica (G4). B) Polarizing light image of the same quartz vein shown above. C) Inset of the SEM-CL image above showing finer texture details. Broken euhedral quartz fragments are visible.

This final stage is much easier to distinguish using SEM-CL observations of vein silica, which allowed the identification of almost the complete evolution only with silica phases; this is particularly useful for samples where boiling textures are cryptic and/or difficult to constrain using an optical microscope (Figure 5).

On the other hand, fluid inclusion assemblages indicate cooling (third to fourth stage) and a late heating event (fourth stage to the present day) in a deep zone. Our new FI data are consistent with those previously published by Sánchez-Alfaro et al. (2016). Moreover, the processes proposed by this study are very similar with those previously described by Sánchez-Alfaro et al. (2016), indicating the utility of SEM-CL imaging, coupled with FI analyses, in the evolution of hydrothermal alteration in active geothermal systems.

Finally, our work shows that studying textural and fluid inclusions petrography, coupled with SEM-CL imaging in carbonate and silica minerals is a useful methodology to decode geothermal systems evolution. Furthermore, quartz, silica polymorphs and carbonates are ubiquitous in geothermal fields, so this methodology has great potential for exploration and understanding of these systems.

6. CONCLUSION

The combination of petrography, FI and SEM-CL analyses in the TGS allow us to confirm the four stages that occur during hydrothermal evolution: 1) flashing, 2) boiling, 3) non-boiling and 4) brecciation of silica minerals due to boiling. The system experienced cooling (S3 to S4) and heating (S4 to now). The processes interpreted by this study are consistent with those proposed by Sánchez-Alfaro et al. (2016), showing the utility of SEM-CL imaging in the characterization of silica textures and identification of other features that can be impossible to see by other more conventional methods.

This work demonstrated that SEM-CL imaging in silica minerals can be a useful methodology to reveal the evolution of hydrothermal systems, and can help in the exploration and understanding of these systems, particularly in those where quartz is the primary and unique mineral present.

ACKNOWLEDGEMENTS

This study has been supported by the CONICYT-FONDAP project 15090013 Andean Geothermal Centre of Excellence (CEGA), grant NC130065 “Millennium Nucleus for Metal Tracing Along Subduction”, and FONDEQUIP EQM 140009 Project. Also, we thank Mighty River Power Chile for field support and access to the drill core samples. We thank Jamie Buscher, Manuel Garcia and Ignacio Villalón for improving the English text.

REFERENCES

Allan, M. and Yardley, B.: Tracking meteoric infiltration into magmatic-hydrothermal system: A cathodoluminescence oxygen isotope and trace element study of quartz from Mt. Leyshon, Australia. *Chemical Geology*. pp. 343 – 360. (2007).

Bignall, G., Sekine, K., Tsuchiya, N.: Fluid-rock interaction processes in the Te Kopia geothermal field (New Zealand) revealed by SEM-CL imaging. *Geothermics*. pp. 615 – 635. (2004).

Dennen, W.H., Blackburn, W.H., Quesada, A.: Aluminium in quartz as a geothermometer. *Contributions to Mineralogy and Petrololy*. pp. 332 – 342. (1970).

Dong, G., Morrison, G., Jaireth, S.: Quartz textures in epithermal veins, Queensland-Classification origin, and implication. *Economic Geology*. pp. 1841 – 1856. (1995).

Dong, G., Zhou, Zoning in the Carboniferous-Lower Permian Cracow epithermal vein system, central Queensland, Australia. *Mineralium Deposits*. pp. 210 – 224. (1996).

Götze, J., Plötze, M., Habermann, D.: Origin, spectral characteristics and practical applications of cathodoluminescence (CL) of quartz-a review. *Mineralogy and Petrology*. pp. 225 – 250. (2001)

Götze, J., Plötze, M., Graupner, T., Hallbauer, D.K., Bray, C.J.: Trace element incorporation into quartz: a combined study by ICP-MS, electron spin resonance, cathodoluminescence, capillary ion analysis, and gas chromatography. *Geochimica et Cosmochimica Acta*. pp. 3741 – 3759. (2004)

Henley, R.W., Hughes, G.O.: Underground fumaroles; “Excess heat” effects in vein formation. *Economic Geology*. pp. 453 – 466. (2000).

Ihinger, P.D., Zink, S.I.: Determination of relative growth rates of natural quartz crystals. *Nature*. pp. 865 – 869. (2000).

Landtwing, M. and Pettke, T.: Relationships between SEM-cathodoluminescence response and trace element composition of hydrothermal vein quartz. *American Mineralogist*. pp. 122 – 131. (2005)

Lohmar, S., Stimac, J., Colvin, A., González, A., Iriarte, S., Melosh, G., Wilmarth, M., Sussman, D.: Tolhuaca volcano (southern Chile, 38.3° latitude S): New learnings from surface mapping and geothermal exploration wells. *XIII Congreso Geológico Chileno, Antofagasta*. pp. 437 – 439. (2012).

Melosh, G., Cumming, W., Benoit, D., Wilmarth, M., Colvin, A., Winick, J., Soto, E., Urzúa, L., Powell, T., Peretz, A., 2010: Exploration results and resource conceptual model of the Tolhuaca Geothermal Field, Chile. *Proceedings World Geothermal Congress* 2010, Indonesia. pp. 25 – 29. (2010).

Melosh, G., Moore, J., Stacey, R.: Natural reservoir evolution in the Tolhuaca geothermal field, southern Chile. *Proceedings, Thirty-Sixth Workshop on Geothermal Reservoir Engineering*, Stanford University, Stanford, California. (2012).

Moncada D., Mutchler S., Nieto A., Reynolds T.J., Rimstidt J.D., Bodnar R.J.: Mineral Textures and Fluid Inclusion Petrography of the Epithermal Ag-Au Deposits at Guanajuato, Mexico. *Journal of Geochemical Exploration*. pp. 20 – 35. (2012).

Monecke, T., Kempe, U., Götze, J: Genetic significance of the trace element content in metamorphic and hydrothermal quartz: a reconnaissance study. *Earth and Planetary Science Letter*. pp. 709 – 724. (2002)

Okamoto, A., Saishu, H., Hirano, N., Tsuchiya, N.: Mineralogical and textural variation of silica minerals in hydrothermal flow-through experiments:

Implications for quartz vein formation. *Geochimica et Cosmochimica Acta*. pp. 3692 – 3706. (2010).

Ramseyer, K. and Müllis, J.: Factors influencing short-lived blue cathodoluminescence of alpha-quartz. *American Mineralogist*. pp. 791 – 800. (1990).

Roedder, E.: Fluid inclusions. *Reviews in Mineralogy*. (1984).

Rogers, A.F.: The occurrence of cristobalite in California. *American Journal of Science*. pp. 222 – 226. (1918).

Sánchez-Alfaro, P., Reich, M., Arancibia, G., Pérez-Flores, P., Cembrano, J., Driesner, T., Lizama, M., Rowland, J., Morata, D., Heinrich, C., Tardani, D., Campos, E.: Physical, chemical and mineralogical evolution of the Tolhuaca geothermal system, southern Andes, Chile: Insights into the interplay between hydrothermal alteration and brittle deformation. *Journal of Volcanology and Geothermal Research.* pp. 88 – 104. (2016).

Simmons, S.F., Christenson, B.W.: Origins of calcite in a boiling geothermal systems. *American Journal of Science.* pp. 361 – 400. (1994).

Sterner, S.M. and Bodnar, R.J.: Synthetic fluid inclusions in natural quartz I. Compostional types synthesized and applications to experimental geochemistry. *Geochimica et Comochimica Acta*. pp. 2659 – 2668. (1984).

Wark, D.A. and Watson, B.E.: TitaniQ: A titanium in quartz geothermometer. *Contributions to Mineralogy and Petrology*. pp.743 – 754. (2006)